

Semiexclusive production of J/ψ mesons in proton-proton collisions with electromagnetic and diffractive dissociation of one of the protons

Anna Cisek,^{1,*} Wolfgang Schäfer,^{2,†} and Antoni Szczurek^{‡2,§}

¹*University of Rzeszów, ul. Rejtana 16, PL-35-959 Rzeszów, Poland*

²*Institute of Nuclear Physics, Polish Academy of Sciences,
ul. Radzikowskiego 152, PL-31-342 Kraków, Poland*

Abstract

We calculate the cross sections for both electromagnetic and diffractive dissociation of protons for semiexclusive production of J/ψ mesons in proton-proton collisions at the LHC. Several differential distributions in missing mass (M_X), or single-particle variables related exclusively to the J/ψ meson are calculated for $\sqrt{s} = 7$ TeV as an example. The cross sections and distributions are compared to the cross section of the purely exclusive reaction $pp \rightarrow ppJ/\psi$. We show the corresponding ratio as a function of J/ψ meson rapidity. We compare the distributions for purely electromagnetic and purely diffractive proton excitations/dissociation. We predict cross sections for electromagnetic and diffractive excitations of similar order of magnitude.

PACS numbers: 13.87.Ce, 14.65.Dw

[‡] also at University of Rzeszów, PL-35-959 Rzeszów, Poland

*Electronic address: acisek@univ.rzeszow.pl

†Electronic address: Wolfgang.Schafer@ifj.edu.pl

§Electronic address: Antoni.Szczurek@ifj.edu.pl

I. INTRODUCTION

Exclusive vector meson production, especially of heavier quarkonia like J/ψ or Y (or their excited states) in $\gamma p \rightarrow Vp$ is generally subjected to pQCD methods. Indeed, the energy dependence of diffractive photoproduction of vector mesons measured at HERA, clearly shows the transition from a soft to hard process, when going from light to heavy vector mesons. Here, for heavy vector mesons, the energy dependence of the diffractive cross section is driven by the gluon distribution of the proton. For a comprehensive review, see ref.[1]. In addition to purely elastic case $\gamma p \rightarrow Vp$ also inelastic $\gamma p \rightarrow VX$ processes with a large rapidity gap between the vector meson and the final state inelastic system X , were observed in experiments performed at HERA [2]. These processes also are of a diffractive nature.

It was realized in last years that the diffractive photoproduction of vector mesons can be studied also in $pp \rightarrow pVp$ processes at the LHC, at even higher energies than were available at HERA. Due account must then be given to absorptive corrections, and interference effects [4, 5].

There has been great interest in the theoretical description of this process. Some authors have suggested to obtain constraints on the collinear glue [6, 7], other works are based on the color dipole approach [8–10], on the k_T -factorization approach [11, 12] with the unintegrated gluon distribution as a basic ingredient. An event generator for central exclusive vector meson production has been recently written [13].

First data at the LHC have been obtained by the LHCb collaboration [14, 15]. The present experimental apparatus was, however, not sufficient to assure full exclusivity. So far in experiments performed e.g. by the LHCb collaboration [14] protons were not measured and only rapidity gaps around vector meson were checked. Therefore the discussed semi-exclusive $\gamma p \rightarrow J/\psi X$ processes may proliferate to the measured cross sections. Some, rather technical, methods were proposed how to eliminate them. However, in order to control the situation better one should understand better those processes on theoretical grounds. In proton-proton collisions two different types of excitation are possible: diffractive as for $\gamma p \rightarrow VX$ and electromagnetic in $p \rightarrow X$ transitions in the vertex with photon exchange.

Diffractive excitation of low mass states is dominated by two phenomena [16, 17].

Firstly, there is the diffractive excitation of positive parity nucleon resonances, a most prominent one being the $N^*(1680)$, $J^P = \frac{5}{2}^+$ state. In addition to the resonance contributions there exists a continuum of πN states diffractively produced via the Drell-Hiida-Deck mechanism. For a recent consideration of this mechanism at LHC energies, see e.g. the discussion of the $pp \rightarrow pp\pi^0$ reaction in [18]. A related hadronic bremsstrahlung mechanism of diffractive production of ωN states has been discussed in [19].

A model for the diffractive excitation of low mass states was considered by Jenkovszky et al. [20] based partially on [21] in a Regge approach. In this approach the resonant contributions dominate.

The large- t continuum was considered in the context of $pp \rightarrow J/\psi X$ reaction. Here perturbative QCD motivated mechanisms, such as those suggested in [22–24] contribute to rather large masses of the diffractively produced system. On the experimental side the H1 collaboration at HERA found comparable cross section for the dissociative processes in $\gamma p \rightarrow J/\psi X$ with respect to the elastic process $\gamma p \rightarrow J/\psi p$ [2]. The large $|t|$ diffractive production of J/ψ mesons in proton-proton collisions was discussed previously in [25]. The authors considered hard Pomeron exchange in a leading-logarithmic BFKL approximation. This process was, however, not discussed there in the context of experimental gaps. In this paper we will show the dependence on the invariant mass of the diffractively produced system, which is closely related to the rapidity gap starting from the vector meson.

As far as electromagnetic excitations are concerned, to our knowledge only the $p \rightarrow \Delta^+$ transition was previously discussed [26] for associated J/ψ and ψ' production. In general, other resonances as well as continuum production may also contribute. Recently we proposed an efficient modeling of such processes in dilepton pair production [27, 28]. The corresponding inelastic cross sections are expressed there in terms of the F_2 structure function. There exist several practical parametrizations of F_2 in different regions of x and Q^2 . The methods used for l^+l^- production can be applied also to $pp \rightarrow pJ/\psi X$ processes discussed here. Preliminary results on the processes with electromagnetic dissociation have been shown in [29].

II. MODELING DISSOCIATIVE PROCESSES

The schematic diagrams of processes considered in this work are shown in Fig.1 for electromagnetic excitation and in Fig.2 for diffractive excitation. In all cases the final state hadronic system can be either a proton resonance or a hadronic/partonic continuum. The details will be given in the following two subsections.

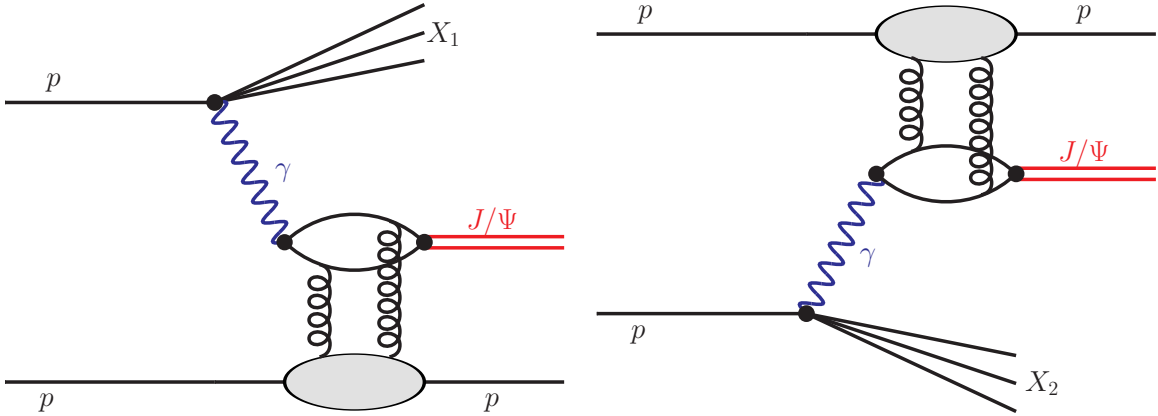


FIG. 1: Schematic representation of the electromagnetic excitation of one (left panel) or second (right panel) proton.

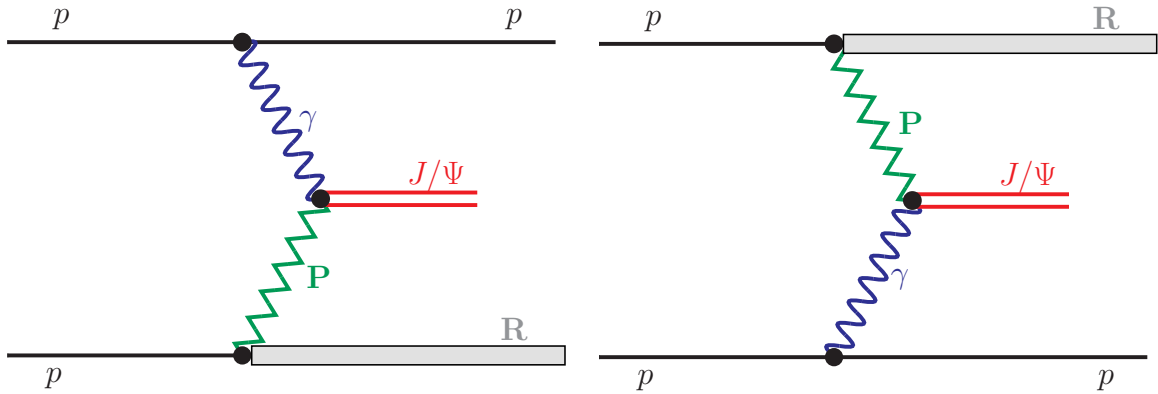


FIG. 2: Schematic representation of the diffractive excitation of one (left panel) or second (right panel) proton.

A. Electromagnetic excitations

Let us first concentrate on the events with electromagnetic dissociation of one of the protons. The important property of these processes is that the $p\gamma^* \rightarrow X$ transition is

given by the electromagnetic structure functions of the proton, and thus to a large extent calculable “from data”. The cross section for such processes can be written as:

$$\frac{d\sigma(pp \rightarrow XVP; s)}{dyd^2\mathbf{p}dM_X^2} = \int \frac{d^2\mathbf{q}}{\pi\mathbf{q}^2} \mathcal{F}_{\gamma/p}^{(\text{inel})}(z_+, \mathbf{q}^2, M_X^2) \frac{1}{\pi} \frac{d\sigma_{\gamma^*p \rightarrow Vp}}{dt}(z_+, s, t = -(\mathbf{q} - \mathbf{p})^2) + (z_+ \leftrightarrow z_-), \quad (2.1)$$

where $z_{\pm} = e^{\pm y} \sqrt{(\mathbf{p}^2 + m_V^2)}/s$. In the kinematics of interest the “fully unintegrated” flux of photons associated with the breakup of the proton is calculable in terms of the structure function F_2 of a proton [27, 28]:

$$\mathcal{F}_{\gamma/p}^{(\text{inel})}(z, \mathbf{q}^2, M_X^2) = \frac{\alpha_{\text{em}}}{\pi} (1-z) \theta(M_X^2 - M_{\text{thr}}^2) \frac{F_2(x_{Bj}, Q^2)}{M_X^2 + Q^2 - m_p^2} \left[\frac{\mathbf{q}^2}{\mathbf{q}^2 + z(M_X^2 - m_p^2) + z^2 m_p^2} \right]^2, \quad (2.2)$$

where

$$Q^2 = \frac{1}{1-z} \left[\mathbf{q}^2 + z(M_X^2 - m_p^2) + z^2 m_p^2 \right], \quad x_{Bj} = \frac{Q^2}{Q^2 + M_X^2 - m_p^2}. \quad (2.3)$$

Often, we are especially interested in the region of small invariant masses, say $M_X \lesssim 2$ GeV, where resonance excitation is important. Our recent study [28] showed, that here it is best to use a parametrization of F_2 given in [30]. For the cross section $\frac{d\sigma_{\gamma^*p \rightarrow Vp}}{dt}$ we employ a parametrization previously used in [5].

B. Diffractive excitations

In distinction to electromagnetic dissociation, which is essentially calculable from data on the electromagnetic structure functions of a nucleon, the diffractive excitation is highly model dependent. Most of the available data were taken at lower energies, see the reviews [16, 17], where the exchange of secondary Regge trajectories is not negligible. There are unfortunately very little data that could be used to constrain the model at LHC energies.

In this exploratory study, we will consider two simple models for the $p\mathbf{IP} \rightarrow X$ transition. The first one will describe the resonance region of $m_p + m_\pi \leq M_X \leq 3 \div 4$ GeV, and is based on a dual Regge approach of [20]. The second approach is based on a parton model description, where the diffractive vector meson production proceeds on a quark or gluon parton of the proton. Here also large diffractive masses M_X are accessible.

1. Resonance excitations

The needed ingredient is the cross section for the diffractive $\gamma p \rightarrow VX$ reaction, where we have a large rapidity gap between the vector meson and the other produced particles.

The large gap is provided by the Pomeron exchange, and we write the cross section in the form

$$\frac{d\sigma(\gamma p \rightarrow VX)}{dt dM_X^2} = \left(\frac{s_{\gamma p}}{M_X^2} \right)^{2\alpha_{\mathbf{P}}^{\text{eff}}(t)-2} \cdot A_0 f_{\gamma \rightarrow V}^2(t) \cdot F(M_X^2, t). \quad (2.4)$$

Here the first factor derives from the propagator of the effective Pomeron, and the constant A_0 fixes the normalization. The function $f_{\gamma \rightarrow V}(t) = \exp[B_{\gamma \rightarrow V} t/2]$ is a formfactor of the $\gamma \rightarrow V$ transition. Finally, the function $F(M_X^2, t)$ contains the information on the dynamics of the diffractive dissociation. Following [20], it reads

$$F(M_X^2, t) = \frac{x(1-x)^2}{(M_X^2 - m_p^2)(1+\tau)^{3/2}} \left(\Im m A(M_X^2, t) + A_{\text{Roper}}(M_X^2, t) \right), \quad (2.5)$$

with

$$x = \frac{|t|}{M_X^2 + |t|}, \quad \tau = \frac{4m_p^2 x^2}{|t|}. \quad (2.6)$$

The contributions of three positive-parity baryon resonances on the nucleon trajectory are taken into account:

1. $N^*(1680)$, $J^P = \frac{5}{2}^+$,
2. $N^*(2220)$, $J^P = \frac{9}{2}^+$,
3. $N^*(2700)$, $J^P = \frac{13}{2}^+$.

Explicitly, they contribute to the $p\mathbf{P} \rightarrow X$ amplitude as:

$$\Im m A(M_X^2, t) = \sum_{n=1,3} [f(t)]^{2(n+1)} \cdot \frac{\Im m \alpha(M_X^2)}{(J_n - \Re e \alpha(M_X^2))^2 + (\Im m \alpha(M_X^2))^2}. \quad (2.7)$$

Here J_n is the spin of the n th resonance, and the explicit form of the complex Regge trajectory $\alpha(M_X^2)$ as well as the formfactor $f(t)$ are found in [20, 31].

Notice that the proton Regge trajectory does not contain the lowest positive-parity excitation of the nucleon, the so-called Roper resonance $N^*(1440)$. Its absence on the

proton trajectory may be related to its structure. In fact there are many indications, that it may be not an ordinary three-quark state [32, 33].

We therefore add by hand a Breit-Wigner term

$$A_{\text{Roper}}(M_X^2, t) = c_{\text{Roper}} f^2(t) \cdot \frac{M_R \Gamma_R}{(M_X^2 - M_R^2)^2 + \Gamma_R^2/4}, \quad (2.8)$$

with $M_R = 1440 \text{ MeV}$, $\Gamma_R = 325 \text{ MeV}$. We fix the normalization of the Roper contribution following ref. [20]. In practice, it turns out however, that the Roper resonance plays only a marginal role.

We can now compute the contribution from diffractive excitation of small masses from the formula

$$\frac{d\sigma(pp \rightarrow XVp; s)}{dy d^2\mathbf{p} dM_X^2} = \int \frac{d^2\mathbf{q}}{\pi \mathbf{q}^2} \mathcal{F}_{\gamma/p}^{(\text{el})}(z_+, \mathbf{q}^2) \frac{1}{\pi} \frac{d\sigma(\gamma p \rightarrow VX)}{dt dM_X^2}(z_+ s) + (z_+ \leftrightarrow z_-), \quad (2.9)$$

with the photon coupling to the elastic leg now given by the well-known electric and magnetic formfactors.

$$\mathcal{F}_{\gamma/p}^{(\text{el})}(z, \mathbf{q}^2) = \frac{\alpha_{\text{em}}}{\pi} (1-z) \left[\frac{\mathbf{q}^2}{\mathbf{q}^2 + z^2 m_p^2} \right]^2 \frac{4m_p^2 G_E^2(Q^2) + Q^2 G_M^2(Q^2)}{4m_p^2 + Q^2}, \quad Q^2 = \frac{\mathbf{q}^2 + z^2 m_p^2}{1-z}. \quad (2.10)$$

2. Partonic continuum

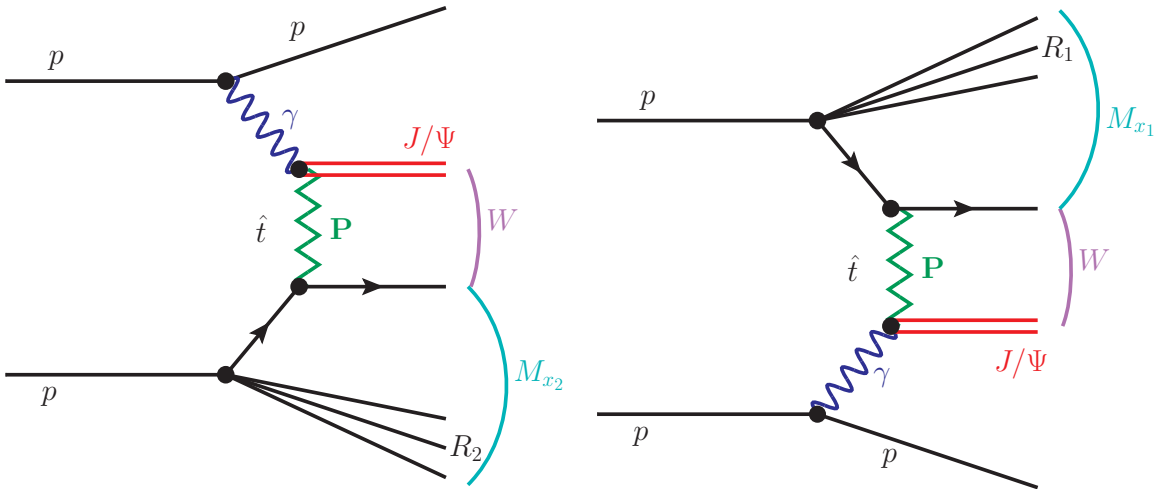


FIG. 3: Schematic representation of the hard diffractive excitation of one (left panel) or second (right panel) proton.

The partonic continuum for the $\gamma p \rightarrow VX$ reaction was discussed in a pedagogical way e.g. in [1]. It will be treated here for the case of proton-proton collisions in a collinear approximation. Schematic diagrams are shown in Fig.3. We shall neglect transverse momenta of the photon and the initial parton. In this approximation the cross section can be written as

$$\begin{aligned} \frac{d\sigma_{pp \rightarrow Vj}^{diff,partonic}}{dy_V dy_j d^2 p_t} &= \frac{1}{16\pi^2 \hat{s}^2} x_1 q_{\text{eff}}(x_1, \mu_F^2) x_2 \gamma_{el}(x_2) \overline{|\mathcal{M}_{q\gamma \rightarrow Vq}|^2} \\ &+ \frac{1}{16\pi^2 \hat{s}^2} x_1 \gamma_{el}(x_1) x_2 q_{\text{eff}}(x_2, \mu_F^2) \overline{|\mathcal{M}_{q\gamma \rightarrow Vq}|^2}. \end{aligned} \quad (2.11)$$

This formula is valid for not too small transverse momenta of the vector meson. The two terms correspond to the two diagrams in Fig.2. The effective parton distribution reads as

$$q_{\text{eff}}(x, \mu_F^2) = \frac{81}{16} g(x, \mu_F^2) + \sum_f \left[q_f(x, \mu_F^2) + \bar{q}_f(x, \mu_F^2) \right]. \quad (2.12)$$

We take $\mu_F^2 = m_V^2 + |\hat{t}|$ for the factorization scale. The matrix element for the partonic subprocess is related to the corresponding \hat{t} -dependence as

$$\frac{d\sigma_{\gamma q \rightarrow Vq}}{d\hat{t}} = \frac{1}{16\pi \hat{s}^2} \overline{|\mathcal{M}_{\gamma q \rightarrow Vq}|^2}. \quad (2.13)$$

The x_1 and x_2 fractions can be calculated from the rapidities and transverse momenta of vector meson y and recoiling parton y_p as

$$x_1 = \sqrt{\frac{m_V^2 + p_T^2}{\hat{s}}} e^y + \frac{p_T}{\sqrt{\hat{s}}} e^{y_p}, \quad x_2 = \sqrt{\frac{m_V^2 + p_T^2}{\hat{s}}} e^{-y} + \frac{p_T}{\sqrt{\hat{s}}} e^{-y_p}. \quad (2.14)$$

The missing mass can be reconstructed from

$$M_X^2 = |\hat{t}| \cdot \frac{1 - x_p}{x_p} + m_p^2, \quad (2.15)$$

where x_p is the momentum fraction carried by the parton.

The matrix element or the corresponding $d\sigma/d\hat{t}$ for the $\gamma + q \rightarrow V + q$ process is the most important ingredient of the whole approach. Different approximations are possible a priori and it is not obvious which approach is the most reliable. Here we use the simplest form motivated by a two-gluon exchange picture.

In the following we shall use a simple formula for two-gluon exchange from Ref.[1] in which the main dependencies on \hat{t} are written explicitly:

$$\frac{d\sigma_{\gamma q \rightarrow Vq}}{d\hat{t}} \propto \alpha_s^2(\bar{Q}_t^2) \alpha_s^2(|\hat{t}|) \frac{m_V^3 \Gamma(V \rightarrow l^+ l^-)}{(\bar{Q}_t^2)^4}, \quad (2.16)$$

where $\bar{Q}_i^2 = m_V^2 + |\hat{t}|$.

We adjust normalization constant to the H1 HERA data [3]. We get a slightly different slope than that in experimental data, but we think such an accuracy is enough for the first estimation of such processes in proton-proton collisions.

Having fixed the normalization constant in Eq.(2.16) we can perform calculations for the proton-proton collisions.

We will be interested in the dependence of the mass of the diffractively excited system M_{X1} for diagram (b) and M_{X2} for diagram (a) that are closely related with the rapidity gaps.

III. NUMERICAL RESULTS

In this section we shall show some differential distributions associated with electromagnetic or diffractive excitation of the final state proton. As an example we shall use two different parametrizations of F_2 , which we denote by FFJLM [30], or ALLM [34], respectively. The first one is adequate for low mass excitations while the applicability of the second one extends to much higher missing masses. We shall consider also both partonic and resonance excitations.

In Fig.4 we start our presentation by showing rapidity distribution of J/ψ meson associated by electromagnetic (left column) and diffractive (right column) excitation of one of the two protons. Contributions of both excitations are shown separately. The second (nonexcited) proton is assumed to be in the ground state. The corresponding contributions are symmetric under $y \rightarrow -y$. Individual contributions (one or second excited proton) has maxima in forward directions (LHCb region).

We show contribution of low-mass electromagnetic excitation (left column) with $M_X < 2, 5, 10$ GeV with FFJLM (solid line) and ALLM (dashed line) parametrizations of the F_2 structure functions. Similarly we show contributions of diffractive (partonic and resonance) contributions (right column). The contributions of electromagnetic excitations (compare left and right columns) are larger than those of the diffractive excitation, which may be surprising at the first look.

In Fig.5 we show the sums of the two single-proton excitations. For comparison we show also contribution of purely exclusive process $pp \rightarrow pJ/\psi p$ (top solid line). We pre-

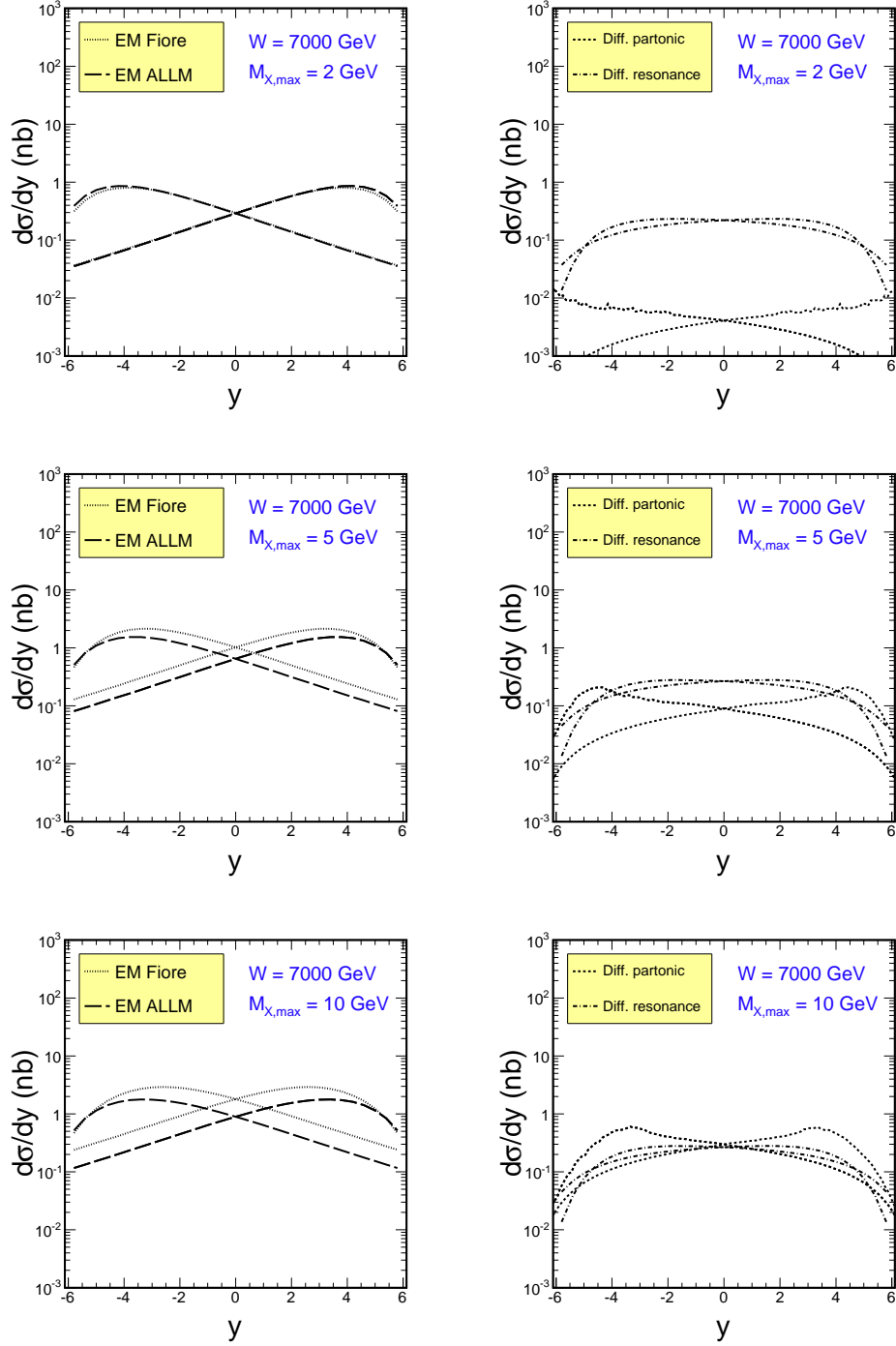


FIG. 4: Rapidity distribution of J/ψ mesons produced when one of the two protons is excited due to photon exchange (left column) and Pomeron exchange (right column).

dict that the contribution of low mass excitations gives camel-like shapes with maxima at $y \approx \pm 4$. When higher (nonresonant) mass region is included the semi-exclusive con-

tribution grows considerably and the two separated maxima merge into one maximum at $y = 0$.

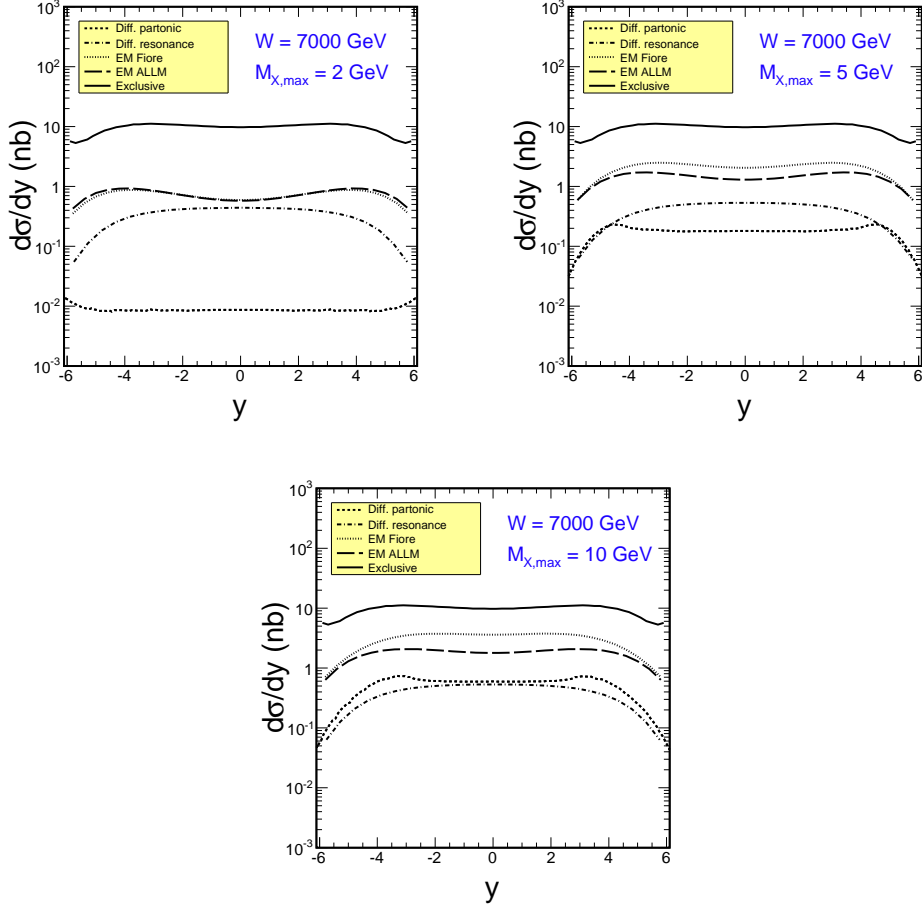


FIG. 5: Rapidity distribution of J/ψ mesons produced when one of the protons is excited due to photon or Pomeron exchange. Both contributions (one or second proton excitation) are added together. We also show a reference distribution for the $pp \rightarrow ppJ/\psi$ exclusive process with parameters taken from [11].

The distribution in missing mass is interesting by itself. In Fig.6 we show distributions in the mass of the excited system (single proton excitation). We show both electromagnetic and diffractive contributions. Again we show result obtained with the FFJLM and ALLM parametrizations of F_2 structure function for the electromagnetic contribution. We can observe that the distributions obtained for the FFJLM and ALLM parametrizations nicely match at $M_X \sim 2$ GeV. Note, that the FFJLM parametrization is reasonable only for $M_X < 2$ GeV while the ALLM parametrization works well in a much broader range of

missing masses M_X [28]. It can be used, in a duality sense, even in the resonance region, if one does not care to resolve the individual resonance contributions.

The diffractive partonic contribution grows gradually with M_X , at least in the region shown in the figure. This means that this contribution is much smaller than its electromagnetic counterpart. One should remember, however, that the electromagnetic contribution contains both resonance and continuum contributions together, while the partonic (continuum) and resonance contributions have been separated for diffractive excitations.

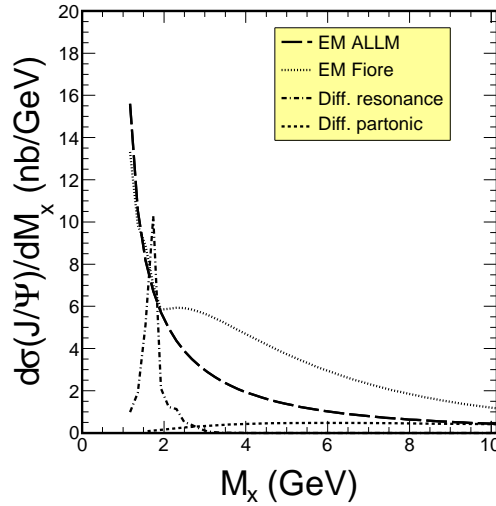


FIG. 6: Distribution in the mass of final state electromagnetic excitation in semiexclusive process of J/ψ mesons production when one of the protons is excited due to photon exchange.

The distribution in transverse momentum of the J/ψ meson is shown in Fig.7. As for the rapidity distribution (see Fig:5) we show the contribution from the low-mass excitation region $M_X < 2, 5, 10$ GeV using the FFJLM or ALLM parametrizations of F_2 . The larger M_X are allowed to contribute, the broader is the distribution in J/ψ transverse momentum. We show also contributions associated with diffractive excitations.

We wish to point out in this context that the LHCb collaboration observed two different slopes in p_T^2 for smaller and larger transverse momenta [14, 15]. It is not clear at this moment whether this is due to a contamination of a purely exclusive component by the semiexclusive contribution discussed here. We also observe two slopes for small and large p_T . A detailed comparison with the LHCb data requires, however, taking into account details of their rapidity gap conditions which in principle requires more detailed

Monte Carlo studies.

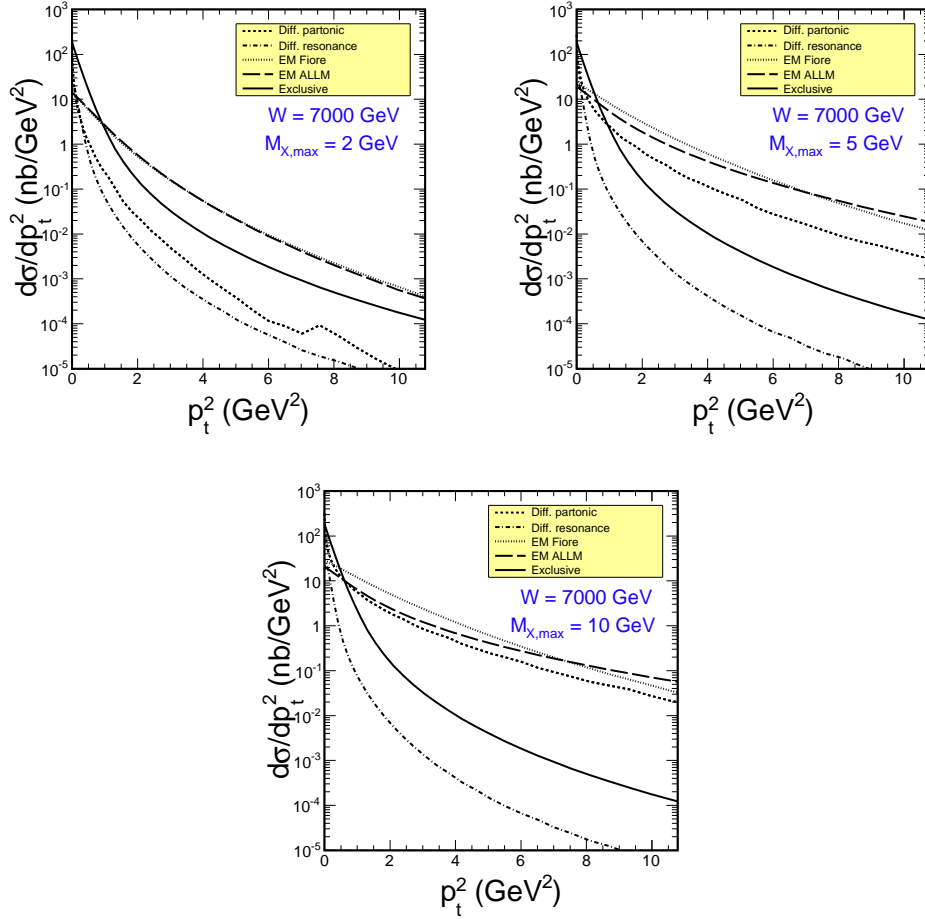


FIG. 7: Transverse momentum distribution of J/ψ mesons. Shown are the cross sections when one of the protons is excited (due to photon or Pomeron exchange). We also show a reference distribution for the $pp \rightarrow ppJ/\psi$ from [11].

When protons are measured one can get insight also into t -distributions. Perhaps this will be soon possible with the help of ALFA/AFP or TOTEM detectors. In the elastic $p \rightarrow p$ transition the t -dependence is governed by the corresponding dependence of the electromagnetic form factor(s) (power-like) for photon exchange or is roughly exponential for soft Pomeron exchange. In Fig.8, we show the distribution in t due to Pomeron exchange on the elastic leg, for the case that the other proton was inelastically excited by the photon exchange. As expected, the dependence is exponential as the proton is emitted from a vertex due to Pomeron exchange.

In the next subsection we wish to compare the several distributions due to electromag-

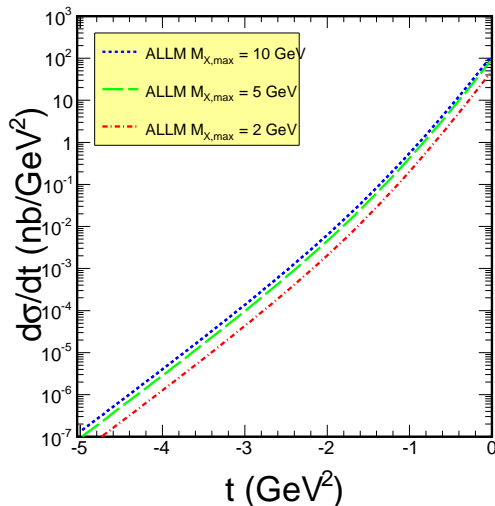


FIG. 8: Distribution in t , the four-momentum transfer squared in the elastic proton leg, associated with J/ψ mesons production when one of the protons is excited due to photon exchange.

netic excitations discussed here with their counterparts due to diffractive excitation.

A. Dissociative processes as a background to purely exclusive process

It is also interesting to see how the cross sections for semiexclusive processes compare to those for the purely exclusive one. We define the following ratio:

$$R(y) = \frac{d\sigma_{pp \rightarrow pJ/\psi X}(M_X < M_{X,\max})/dy}{d\sigma_{pp \rightarrow pJ/\psi p}/dy}. \quad (3.1)$$

This ratio is shown in Fig.9 for three different values of $M_{X,\max}$. We see that the magnitude as well as the shape of the ratio depends on the range of missing masses included in the calculation.

B. Predictions for LHCb

Here we wish to show predictions of our calculations for LHCb cuts. The LHCb collaboration is the only one which measures “semiexclusive” production of J/ψ mesons at the LHC. However, so far it was not possible to assure full exclusivity. The LHCb collaboration imposes a condition on rapidity gaps in forward directions. The large rapidity gaps means automatically low-mass excitations. In Fig.10 we show transverse momentum dis-

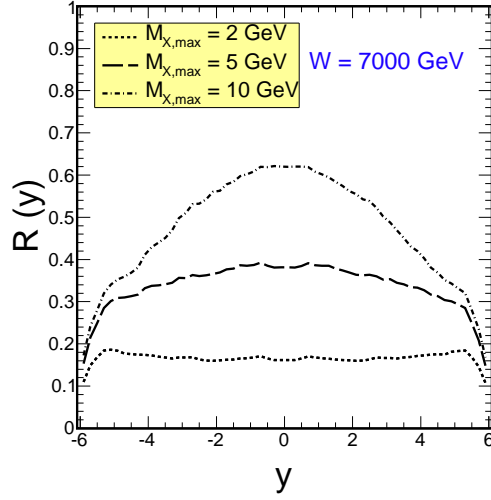


FIG. 9: $R(y)$ as a function of J/ψ rapidity for different ranges of M_X . Both electromagnetic and diffractive excitations are included here.

tribution of J/ψ meson for different ranges of proton excitations ($M_X < 2, 5$ and 10 GeV for the three panels). The larger masses of the proton excitations the larger slopes of the transverse momentum distribution of J/ψ . For comparison we show distribution for purely exclusive case. The inelastic contributions start to dominate over the purely elastic (exclusive) contribution for $p_T > 1$ GeV. How the maximal mass of proton excitation translates to rapidity gap requires a dedicated Monte Carlo study which goes, however, beyond the scope of the present paper. On the experimental side, the LHCb collaboration could study modification of the transverse momentum distribution of J/ψ when modifying the size of rapidity gap. When combined with the Monte Carlo simulation it would allow for studying the contribution of semi-exclusive processes.

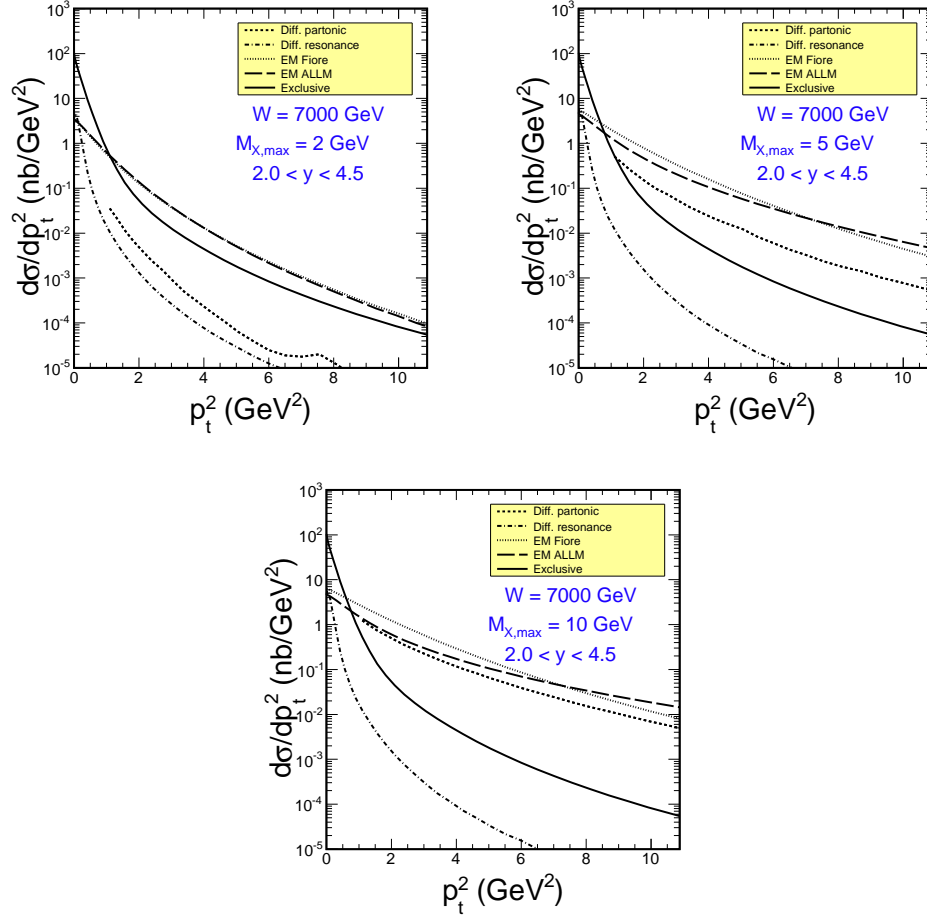


FIG. 10: Transverse momentum distribution of J/ψ mesons produced when one of the protons is excited due to photon or Pomeron exchange. In this calculation we have taken into account restrictions in rapidity relevant for the LHCb experiment. We also show a reference distribution for the $pp \rightarrow ppJ/\psi$ using parameters from [11].

IV. CONCLUSIONS

In the present paper we have discussed the semi-exclusive production of J/ψ mesons allowing both for electromagnetic and diffractive excitation/dissociation of one of the colliding protons.

The electromagnetic excitations were treated as proposed recently for semiexclusive production of dilepton pairs including transverse momenta of virtual photons. This method allows to control therefore transverse momenta of the associated J/ψ mesons.

As far as diffractive excitations are considered we have included two mechanisms of

low-mass soft excitation as proposed some time ago for single diffraction excitation and partonic continuum dissociation mechanism discussed previously in the context of large- t production of vector mesons in inelastic processes of the type $\gamma p \rightarrow VX$ with rapidity gap.

Several differential distributions in rapidity and transverse momentum of the J/ψ meson, in mass of the excited proton-like system and in four-momentum transfer squared have been presented both for the electromagnetic and diffractive excitations. We have compared the corresponding contributions. The electromagnetic-dissociation contribution is in general larger than the diffractive-dissociation one.

In addition, we have calculated ratios of contribution for inelastic (electromagnetic or diffractive) processes to the purely exclusive one ($pp \rightarrow ppJ/\psi$) as a function of J/ψ rapidity. An interesting pattern has been obtained which could be verified in the future.

Some predictions for the LHCb kinematics have been presented. Measurable cross sections have been obtained. We have suggested that a measurement of the semi-exclusive excitation by the LHCb collaboration is possible and could be done in a near future.

Acknowledgments

We would like to thank Ronan McNulty and Tomasz Szumlak for discussion of the possibility of a measuring the here discussed processes at LHCb. This study was partially supported by the Polish National Science Center grant DEC-2014/15/B/ST2/02528 and by the Center for Innovation and Transfer of Natural Sciences and Engineering Knowledge in Rzeszów.

-
- [1] I. P. Ivanov, N. N. Nikolaev and A. A. Savin, *Phys. Part. Nucl.* **37** (2006) 1 [hep-ph/0501034].
 - [2] C. Alexa *et al.* [H1 Collaboration], *Eur. Phys. J. C* **73**, no. 6, 2466 (2013) [arXiv:1304.5162 [hep-ex]].
 - [3] A. Aktas *et al.* [H1 Collaboration], *Phys. Lett. B* **568**, 205 (2003) [hep-ex/0306013].
 - [4] S. R. Klein and J. Nystrand, *Phys. Rev. Lett.* **92**, 142003 (2004) [hep-ph/0311164].
 - [5] W. Schäfer and A. Szczurek, *Phys. Rev.* **D76** (2007) 094014.
 - [6] S. P. Jones, A. D. Martin, M. G. Ryskin and T. Teubner, *JHEP* **1311**, 085 (2013) [arXiv:1307.7099].

- [hep-ph]].
- [7] V. P. Goncalves, L. A. S. Martins and W. K. Sauter, *Eur. Phys. J. C* **76**, no. 2, 97 (2016) [arXiv:1511.00494 [hep-ph]].
- [8] L. Motyka and G. Watt, *Phys. Rev. D* **78**, 014023 (2008) [arXiv:0805.2113 [hep-ph]].
- [9] M. B. Gay Ducati, M. T. Griep and M. V. T. Machado, *Phys. Rev. D* **88**, 017504 (2013) [arXiv:1305.4611 [hep-ph]].
- [10] V. P. Goncalves, B. D. Moreira and F. S. Navarra, *Phys. Rev. C* **90**, no. 1, 015203 (2014) [arXiv:1405.6977 [hep-ph]].
- [11] A. Cisek, W. Schäfer and A. Szczurek, *JHEP* **1504** (2015) 159.
- [12] I. Bautista, A. Fernandez Tellez and M. Hentschinski, *Phys. Rev. D* **94**, no. 5, 054002 (2016) [arXiv:1607.05203 [hep-ph]].
- [13] G. G. da Silveira, V. P. Goncalves and M. M. Jaime, arXiv:1609.09854 [hep-ph].
- [14] R. Aaij *et al.* [LHCb Collaboration], *J. Phys. G* **40** (2013) 045001 [arXiv:1301.7084 [hep-ex]].
- [15] R. Aaij *et al.* [LHCb Collaboration], *JHEP* **1509** (2015) 084 [arXiv:1505.08139 [hep-ex]].
- [16] G. Alberi and G. Goggi, *Phys. Rept.* **74**, 1 (1981).
- [17] N. P. Zotov and V. A. Tsarev, *Sov. Phys. Usp.* **31**, 119 (1988).
- [18] P. Lebiedowicz and A. Szczurek, *Phys. Rev.* **D87** (2013) 074037.
- [19] A. Cisek, P. Lebiedowicz, W. Schäfer and A. Szczurek, *Phys. Rev. D* **83**, 114004 (2011) [arXiv:1101.4874 [hep-ph]].
- [20] L.L. Jenkovszky, O.E. Kuprash, J.W. Lamsa, V.K. Magas and R. Orava, *Phys. Rev.* **D83** (2011) 056014.
- [21] G. A. Jaroszkiewicz and P. V. Landshoff, *Phys. Rev. D* **10**, 170 (1974).
- [22] J. R. Forshaw and M. G. Ryskin, *Z. Phys. C* **68**, 137 (1995) [hep-ph/9501376].
- [23] R. Enberg, J.R. Forshaw, L. Motyka and G. Poludniowski, *JHEP*0309 (2003) 008.
- [24] G.G. Poludniowski, R. Enberg, J.R. Forshaw and L. Motyka, *JHEP*0312 (2003) 002.
- [25] V. P. Goncalves and W. K. Sauter, *Phys. Rev.* **D81** 074028 (2010).
- [26] V. Guzey and M. Zhalov, arXiv:1405.7529.
- [27] G. G. da Silveira, L. Forthomme, K. Piotrkowski, W. Schäfer and A. Szczurek, *JHEP* **1502** (2015) 159 [arXiv:1409.1541 [hep-ph]].
- [28] M. Łuszczak, W. Schäfer and A. Szczurek, *Phys. Rev. D* **93** (2016) no.7, 074018 [arXiv:1510.00294 [hep-ph]].

- [29] W. Schäfer, A. Szczurek and A. Cisek, PoS DIS **2016**, 205 (2016) [arXiv:1607.00900 [hep-ph]].
- [30] R. Fiore, A. Flachi, L. L. Jenkovszky, A. I. Lengyel and V. K. Magas, Eur. Phys. J. A **15** (2002) 505 [hep-ph/0206027].
- [31] R. Fiore, L. L. Jenkovszky, F. Paccanoni and A. Prokudin, Phys. Rev. D **70**, 054003 (2004) [hep-ph/0404021].
- [32] O. Krehl, C. Hanhart, S. Krewald and J. Speth, Phys. Rev. C **62**, 025207 (2000) [nucl-th/9911080].
- [33] I. T. Obukhovskiy, A. Faessler, T. Gutsche and V. E. Lyubovitskij, Phys. Rev. D **89**, no. 1, 014032 (2014) [arXiv:1306.3864 [hep-ph]].
- [34] H. Abramowicz, E. M. Levin, A. Levy and U. Maor, Phys. Lett. B **269**, 465 (1991); H. Abramowicz and A. Levy, hep-ph/9712415.